

# Two New Red/Near-Infrared Ir(III) Complexes with Reversible and Force-Induced Enhanced Mechanoluminescence

Yuzhen Yang, Qin Zeng, Weiqiao Zhou, Junjie Jiang, Zihao Zhang, Song Guo \* and Yuanli Liu \*

Guangxi Key Laboratory of Optical and Electronic Materials and Devices, College of Materials Science and Engineering, Guilin University of Technology, Guilin 541004, China; yangyuzhen812@163.com (Y.Y.); zqinnn@163.com (Q.Z.); wangyi123zhou@163.com (W.Z.); jiejiangjj0513@163.com (J.J.); 1020190104@glut.edu.cn (Z.Z.)

\* Correspondence: bobingjin@glut.edu.cn (S.G.); lyuanli@glut.edu.cn (Y.L.)

## 1. General Experimental Information

The NMR spectra were measured on Bruker Avance 500 MHz with tetramethylsilane as the internal standard. Mass spectra were obtained on Bruker matrix-assisted laser desorption/ionization time-of-flight mass spectrometer (MALDI-TOF-MASS). The UV–Vis absorption spectrum was recorded on a Lambda 750 spectrometer (PerkinElmer, America). Emission spectra and lifetimes were measured on a FluoroMax-4 fluorescence spectrophotometer (Horiba, Japan). The excited-state lifetime was measured on a transient spectro-fluorimeter (Edinburgh QM 8000) with a time-correlated single-photon counting technique. Photographs were taken using Canon 90D camera (Canon, Japan). Cyclic voltammetry was performed on the IVIUMSTAT.h instrument with a scan rate of 100 mV s<sup>−1</sup> in CH<sub>2</sub>Cl<sub>2</sub> solutions, a glassy-carbon electrode as the working electrode, an aqueous saturated potassium chloride electrode as the pseudo-reference electrode, and a platinum wire as the counter electrode, respectively. A 0.1 M solution of tetrabutylammonium hexafluorophosphate in CH<sub>2</sub>Cl<sub>2</sub> was used as the supporting electrolyte, and the ferrocene/ferrocenium (Fc<sup>+</sup>/Fc) potential was measured and selected as the internal standard. Powder X-ray diffraction of original and mechanically ground forms were measured in PANalytical diffractometer.

## 2. Calculation method

The ground-state geometrical configuration was optimized by density functional theory (DFT) with B3LYP functional. Based on the optimized ground state molecular structure, the time-dependent DFT (TDDFT) approach associated with the polarized continuum model (PCM) in dichloromethane media was carried out to

obtain the vertical excitation energies of triplet states ( $T_n$ ). The calculation was performed using the Gaussian 16 B.01 suite of programs. The SDD basis set was used to treat the iridium atom, whereas the 6-31G\* basis set was used to treat all other atoms. The contours of the highest occupied molecular orbital (HOMO) and lowest unoccupied molecular orbital (LUMO) were plotted using Multiwfn 3.8 soft. <sup>[S1-2]</sup>

### 3. Synthesis of cyclometalating ligand and Iridium(III) Complexes

Synthetic routes of **Ir1** and **Ir2** are described in **Figure 1**.

Synthesis of main ligand **2**:

*2-Boronate anthraquinone (1)*. 2-bromoanthraquinone (2.0 g, 7.0 mmol), bis(pinacolato)diboron (2.1 g, 7.0 mmol), and [1,1'-bis(diphenylphosphino)ferrocene]dichloropalladium(II) (complex with dichloromethane) (0.3 g, 0.35 mmol) were dissolved in 30 mL 1,4-dioxane, and 10 equivalent KAc was added. The mixture was refluxed at 100°C under a nitrogen atmosphere for 24 h. After that, the resulting precipitate was discarded using filtration, and the filtrate was extracted with CH<sub>2</sub>Cl<sub>2</sub> and water several times. Then, the organic layer was dried over anhydrous Na<sub>2</sub>SO<sub>4</sub>, filtered, and concentrated. Finally, the residue was purified using column chromatography (silica, dichloromethane/petroleum ether = 1:2) and yielded a pale-yellow powder **1** (yield: 70%). <sup>1</sup>H NMR (500 MHz, Chloroform-d)  $\delta$  8.75 (s, 1H, arom. C<sub>6</sub>H<sub>3</sub>), 8.36 – 8.26 (m, 3H, arom. C<sub>6</sub>H<sub>4</sub>), 8.20 (d,  $J$  = 7.6 Hz, 1H, arom. C<sub>6</sub>H<sub>3</sub>), 7.84 – 7.76 (m, 2H), 1.38 (s, 13H, CH<sub>3</sub> groups).

*2-(1-isoquinoliny)-9,10-anthraquinone (2)*. The precursor 2-boronate anthraquinone (1.0 g, 3.0 mmol), 1-chloroisoquinoline (0.5 g, 3.0 mmol), and tetrakis(triphenylphosphine)palladium (0.1 g, 0.09 mmol) were dissolved in the mixture of toluene, ethanol, and water (V:V:V = 3:1:1, 40 mL), and 10 equivalent K<sub>2</sub>CO<sub>3</sub> was added. The mixture was refluxed at 95°C under a nitrogen atmosphere for 12 h. The post-processing was similar to that of **1**. The yellow product **2** was collected and dried overnight (yield: 70%). <sup>1</sup>H NMR (500 MHz, Chloroform-d)  $\delta$  8.68 (d,  $J$  = 8.6 Hz, 2H), 8.51 (d,  $J$  = 7.9 Hz, 1H), 8.42 – 8.29 (m, 2H), 8.19 (d,  $J$  = 8.0 Hz, 1H), 8.06 (d,  $J$  = 8.5 Hz, 1H), 7.96 (d,  $J$  = 8.1 Hz, 1H), 7.87 – 7.81 (m, 2H), 7.76 (t,  $J$  = 5.4 Hz, 2H), 7.61 (t,  $J$  = 7.6 Hz, 1H).

Synthesis of the chloro-bridged dimer **3**:

The dimer **3** was synthesized from a reaction of IrCl<sub>3</sub> • 3H<sub>2</sub>O (0.26 g, 0.75 mmol) with 2-(1-isoquinoliny)-9,10-anthraquinone (0.5 g, 1.5 mmol) in the mixture of 2-ethoxyethanol and water mixture (V:V = 3:1, 40 mL)

at 110°C under nitrogen atmosphere for 24 h. After cooling to room temperature, excess water was added into the mixture to induce precipitation. The precipitate was filtered and dried overnight.

#### Synthesis of Iridium(III) Complex:

The synthesis of **Ir1** and **Ir2** is according to a previously reported method. [S3-6]

*Synthesis and characterization of complex Ir1.* Chloro-bridged dimer **3** (0.1 g, 0.08 mmol) and 4,4'-dimethyl-2,2'-bipyridyl (0.03 g, 0.16 mmol) were dissolved in the mixture of dichloromethane and methanol (V:V = 3:1, 32 mL), and 5 equivalent KPF<sub>6</sub> was added, and then the solution was refluxed at 40°C for 5 h. The mixture was extracted with CH<sub>2</sub>Cl<sub>2</sub> and water several times to collect the organic phase that was dried over anhydrous Na<sub>2</sub>SO<sub>4</sub>, filtered, and concentrated. The crude product was purified with column chromatography (neutral alumina, dichloromethane/methanol = 100:1) to yield a deep-red powder **Ir1** (yield: 66%). <sup>1</sup>H NMR (500 MHz, Chloroform-d) δ 9.91 (s, 2H, arom. C<sub>5</sub>H<sub>2</sub>), 9.23 (s, 2H, arom. C<sub>5</sub>H<sub>2</sub>), 9.11 (d, J = 8.3 Hz, 2H), 8.28 (d, J = 7.6 Hz, 2H), 8.06 (s, 4H), 7.98 (t, J = 7.05 Hz, 2H), 7.93 (t, J = 7.05 Hz, 2H), 7.75 (t, J = 7.45 Hz, 2H), 7.70 (t, J = 7.55 Hz, 2H), 7.60 (m, J = 7.6 Hz, 4H), 7.55 (d, J = 6.2 Hz, 2H), 7.13 (d, J = 5.1 Hz, 2H), 2.71 (s, 6H, CH<sub>3</sub> groups). <sup>13</sup>C NMR (126 MHz, Chloroform-d) δ 183.26, 183.18, 166.30, 163.68, 155.48, 154.01, 151.79, 148.57, 140.27, 137.32, 134.19, 133.99, 133.76, 133.30, 132.67, 132.43, 130.35, 129.69, 129.14, 129.03, 128.17, 127.16, 127.03, 126.93, 126.30, 124.45, 29.70, 21.56. <sup>19</sup>F NMR (471 MHz, Chloroform-d) δ -72.83 (d, J = 711.21 Hz) <sup>31</sup>P NMR (202 MHz, Chloroform-d) δ -144.67 (sep, J = 713.06 Hz). MALDI-TOF-MS (m/z): calcd. for C<sub>58</sub>H<sub>36</sub>IrN<sub>4</sub>O<sub>4</sub>, 1045.17; found, 1044.752. The related complex **Ir2** was prepared using similar procedures.

**Ir2:** deep-red powder (62% yield). <sup>1</sup>H NMR (500 MHz, Chloroform-d) δ 9.35 (s, 2H, arom. C<sub>5</sub>H<sub>2</sub>), 9.23 (s, 2H, arom. C<sub>5</sub>H<sub>2</sub>), 9.11 (d, J = 8.5 Hz, 2H), 8.27 (d, J = 7.5 Hz, 2H), 8.06 (t, J = 6.7 Hz, 4H), 7.98 (t, J = 8.2 Hz, 2H), 7.94 (t, J = 7.25 Hz, 2H), 7.74 (t, J = 7.4 Hz, 2H), 7.70 (t, J = 7.3 Hz, 2H), 7.63 (m, 4H), 7.50 (d, J = 6.4 Hz, 2H), 6.79 (d, J = 5.8 Hz, 2H), 4.41 (s, 6H, OCH<sub>3</sub> groups). <sup>13</sup>C NMR (126 MHz, Chloroform-d) δ 183.27, 183.16, 168.96, 166.34, 164.17, 158.10, 151.85, 149.55, 140.33, 137.27, 134.15, 133.95, 133.74, 133.27, 132.60, 132.37, 130.28, 129.70, 129.01, 128.16, 128.13, 127.12, 126.98, 126.89, 126.28, 124.37, 116.80, 112.13, 59.17, 30.94, 29.69, 29.61, 29.52, 29.31, 29.20, 21.22, 14.18. <sup>19</sup>F NMR (471 MHz, Chloroform-d) δ -72.64 (d, J = 711.21 Hz). <sup>31</sup>P NMR (202 MHz, Chloroform-d) δ -144.44 (sep, J = 711.04 Hz). MALDI-TOF-MS (m/z): calcd. for C<sub>58</sub>H<sub>36</sub>IrN<sub>4</sub>O<sub>6</sub>, 1077.18; found, 1076.729.

## References

- [S1] Frisch, M.J.; Trucks, G.W.; Schlegel, H.B.; Scuseria, G.E.; Robb, M.A.; Cheeseman, J.R.; Scalmani, G.; Barone, V.; Petersson, G.A.; Nakatsuji, H.; Li, X.; Caricato, M.; Marenich, A.V.; Bloino, J.; Janesko, B.G.; Gomperts, R.; Mennucci, B.; Hratchian, H.P.; Ortiz, J.V.; Izmaylov, A.F.; Sonnenberg, J.L.; Williams, Ding, F.; Lipparini, F.; Egidi, F.; Goings, J.; Peng, B.; Petrone, A.; Henderson, T.; Ranasinghe, D.; Zakrzewski, V.G.; Gao, J.; Rega, N.; Zheng, G.; Liang, W.; Hada, M.; Ehara, M.; Toyota, K.; Fukuda, R.; Hasegawa, J.; Ishida, M.; Nakajima, T.; Honda, Y.; Kitao, O.; Nakai, H.; Vreven, Y.; Throssell, K.; Montgomery J, J.A.; Peralta, J.E.; Ogliaro, F.; Bearpark, M.J.; Heyd, J.J.; Brothers, E.M.; Kudin, K.N.; Staroverov, V.N.; Keith, T.A.; Kobayashi, R.; Normand, J.; Raghavachari, K.; Rendell, A.P.; Burant, J.C.; Iyengar, S.S.; Tomasi, J.; Cossi, M.; Millam, J.M.; Klene, M.; Adamo, C.; Cammi, R.; Ochterski, J.W.; Martin, R.L.; Morokuma, K.; Farkas, O.; Foresman, J.B.; Fox, D.J.; Wallingford. CT. 2016.
- [S2] Lu, T.; Chen F. W. Multiwfn. J. Comput. Chem. 2012, 33, 580-592.
- [S3] Guo, S.; Guo, C. X.; Lu, Z.; Du, L. L.; Gao, M.; Liu, S. J.; Liu, Y. L.; Zhao, Q. Crystals. 2021, 11, 1190.
- [S4] Sun, H. B.; Liu, S. J.; Lin, W. P.; Zhang, K. Y.; Lv, W.; Huang, X.; Huo, F. W.; Yang, H. R.; Jenkins, G.; Zhao, Q.; Huang, W.. Nat. Commun. 2014, 5, 3601.
- [S5] Tao, P.; Li, W. L.; Zhang, J.; Guo, S.; Zhao, Q.; Wang, H.; Wei, B.; Liu, S. J.; Zhou, X. H.; Yu, Q.; Xu, B. S.; Huang, W. Adv. Funct. Mater. 2016, 26, 881.
- [S6] Nonoyama, M. Bull. Chem. Soc. Jpn. 1974, 47, 767.

## NMR and MS Spectra

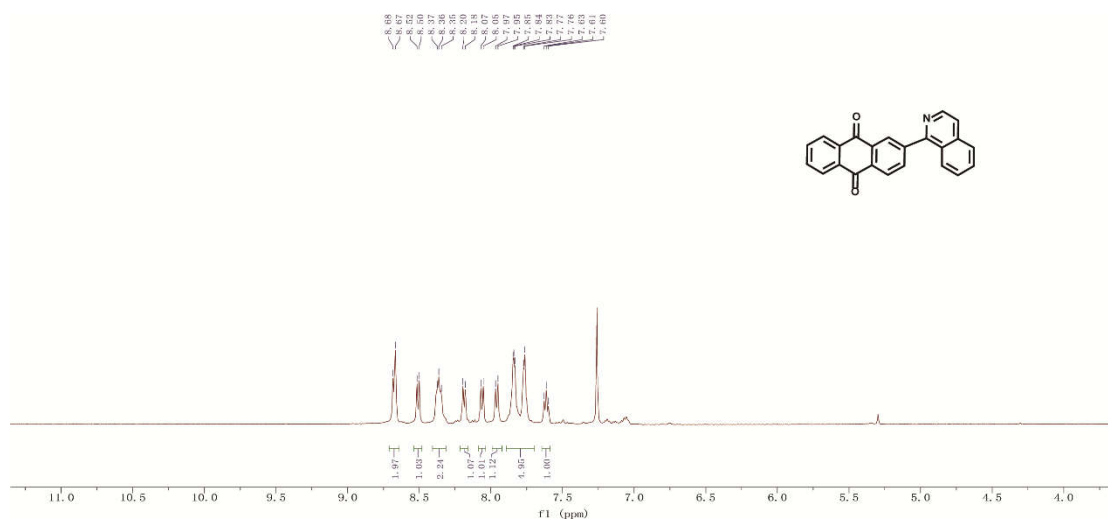


**Figure S1.** The  $^1\text{H}$  NMR spectrum of the main ligand **2**.

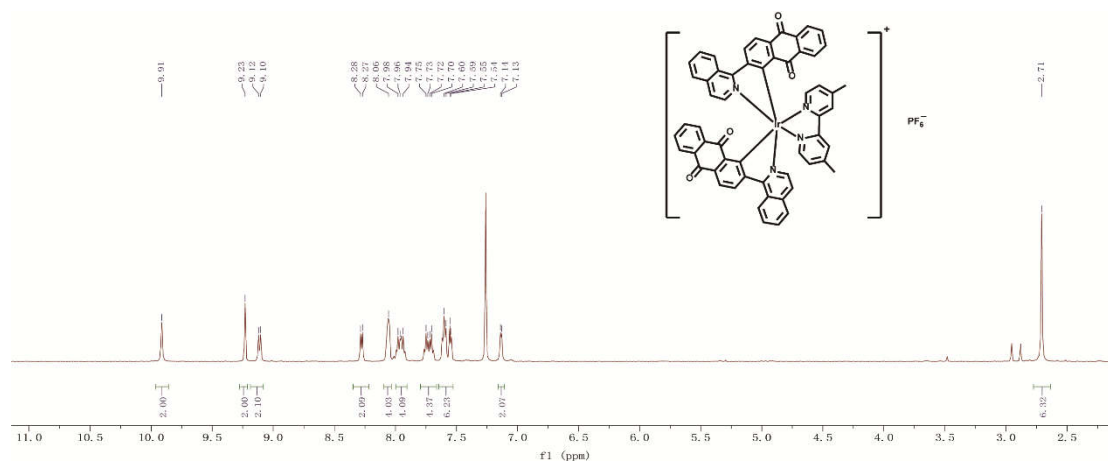


**Figure S2.** The  $^1\text{H}$  NMR spectrum of complex **Ir1**.

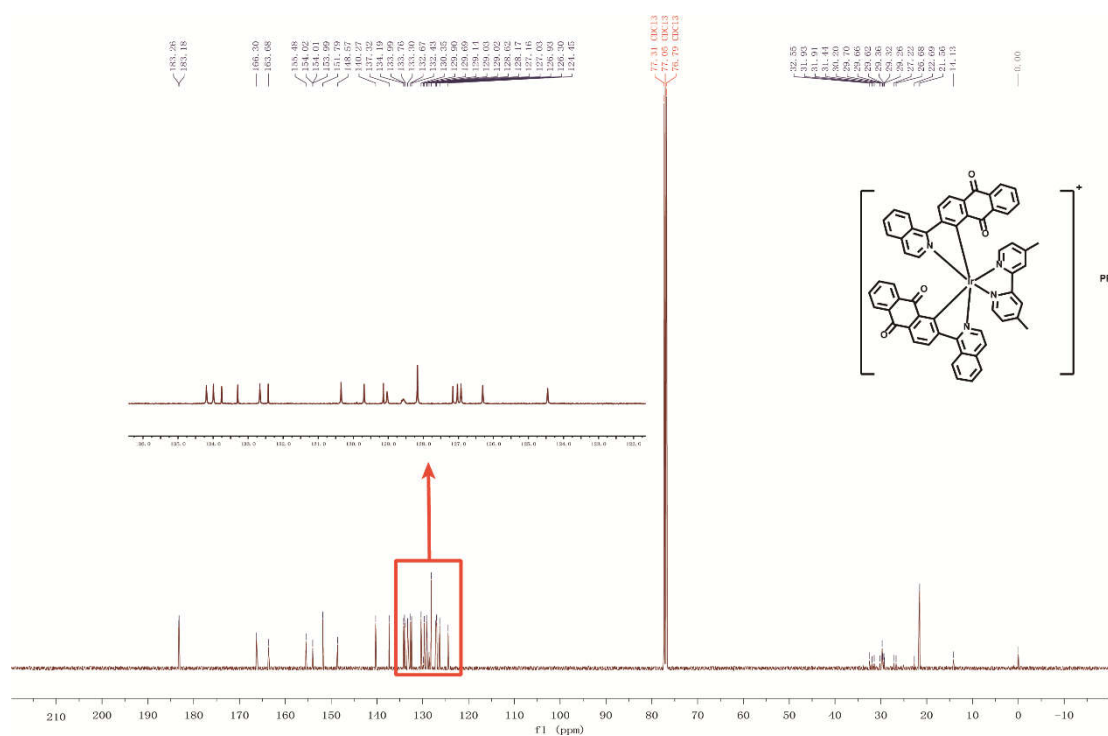


**Figure S3.** The  $^{13}\text{C}$  NMR spectrum of complex **Ir1**.

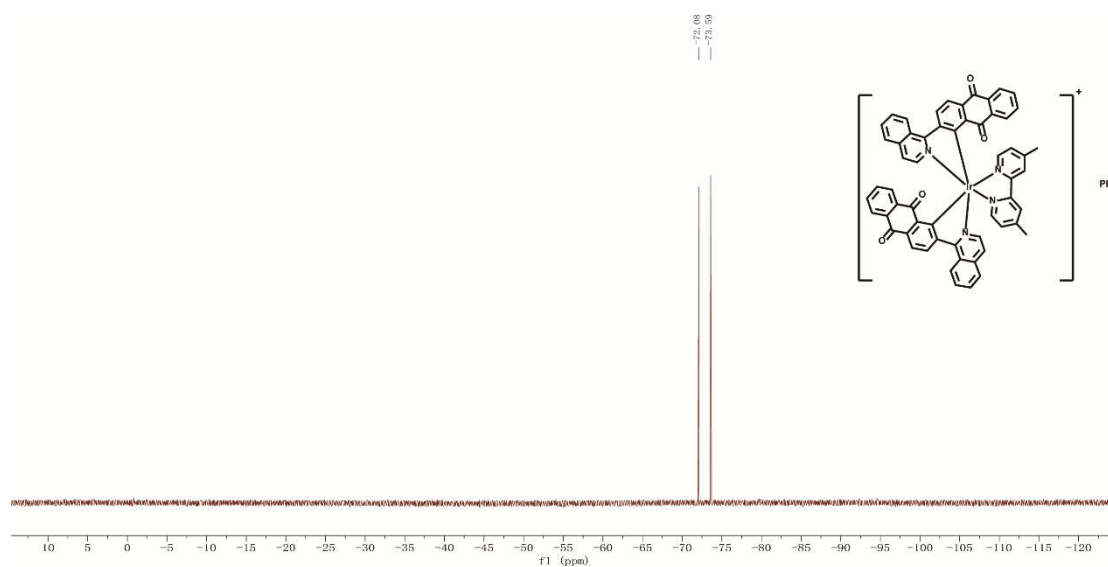


**Figure S4.** The  $^{19}\text{F}$  NMR spectrum of complex **Ir1**.

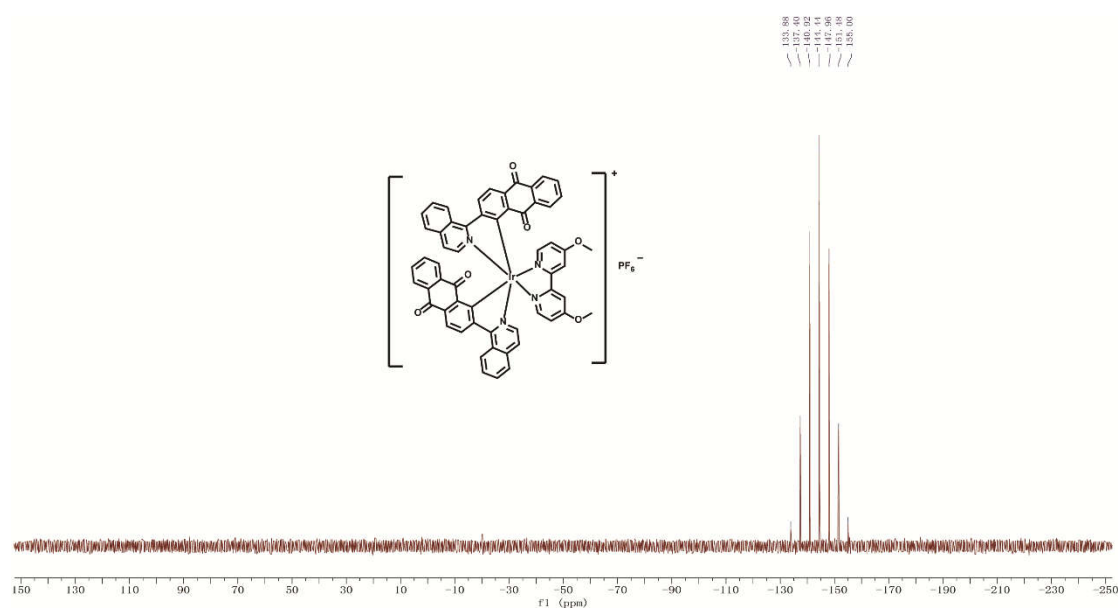


Figure S5. The <sup>31</sup>P NMR spectrum of complex Ir1.

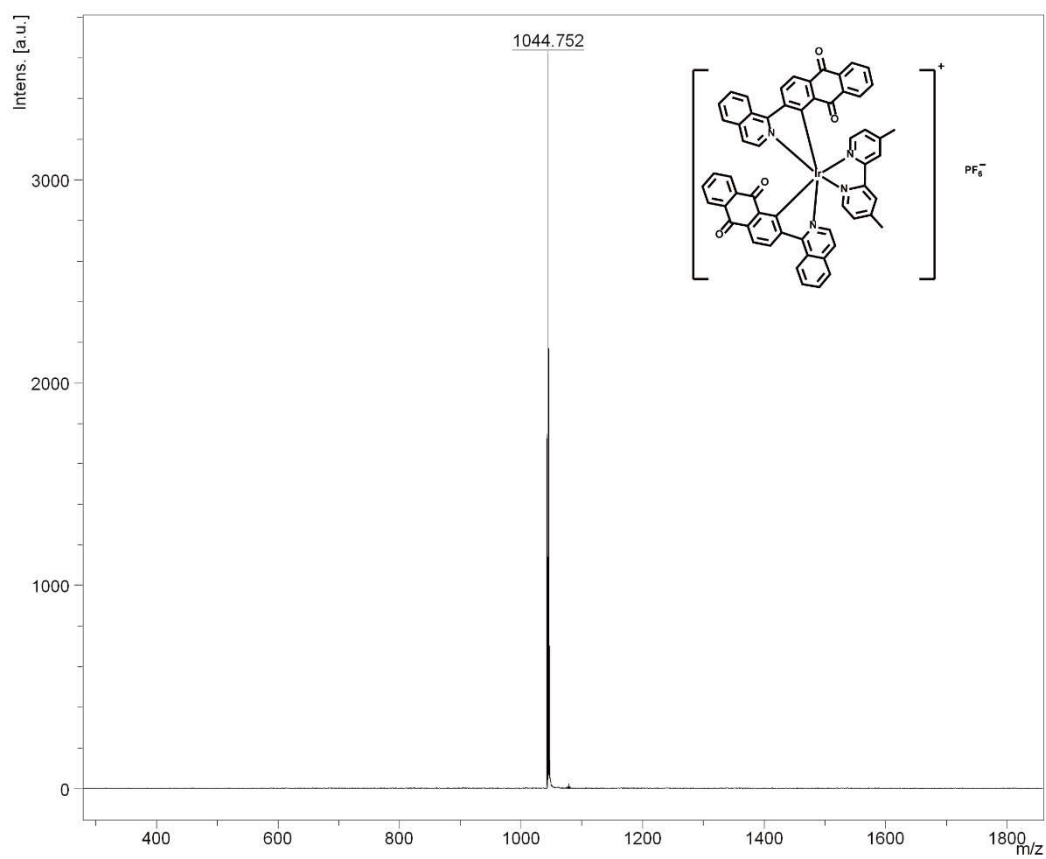


Figure S6. MALDI-TOF spectrum of complex Ir1.

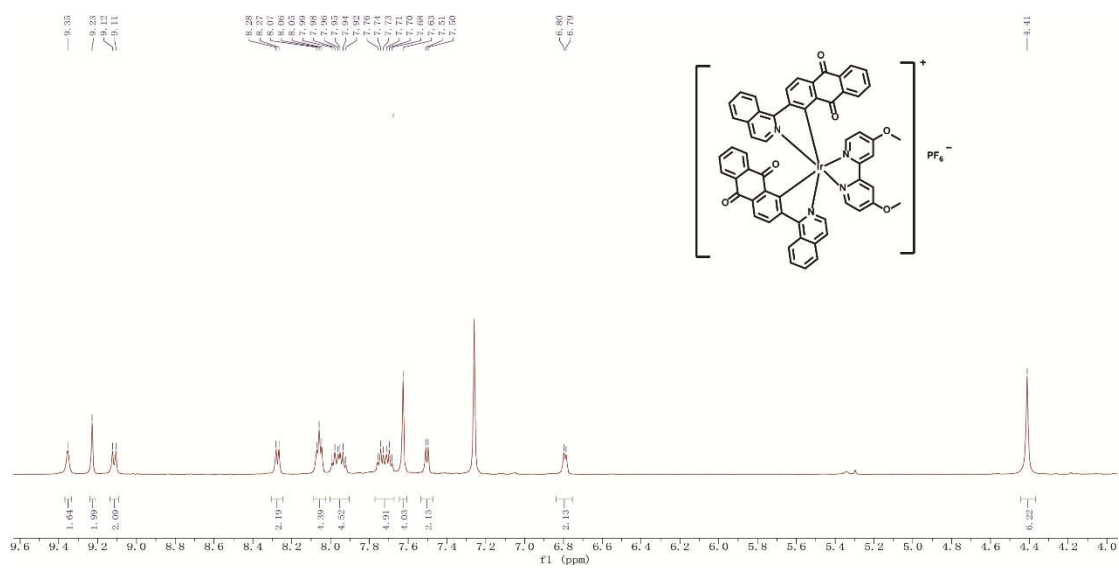


Figure S7. The  $^1\text{H}$  NMR spectrum of complex **Ir2**.

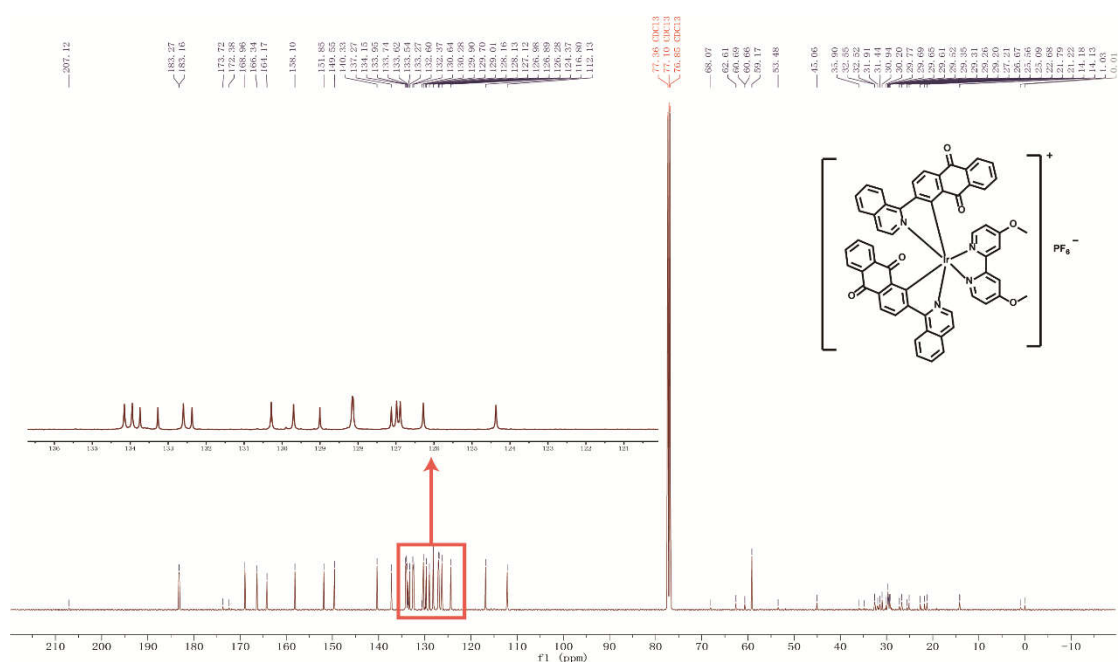
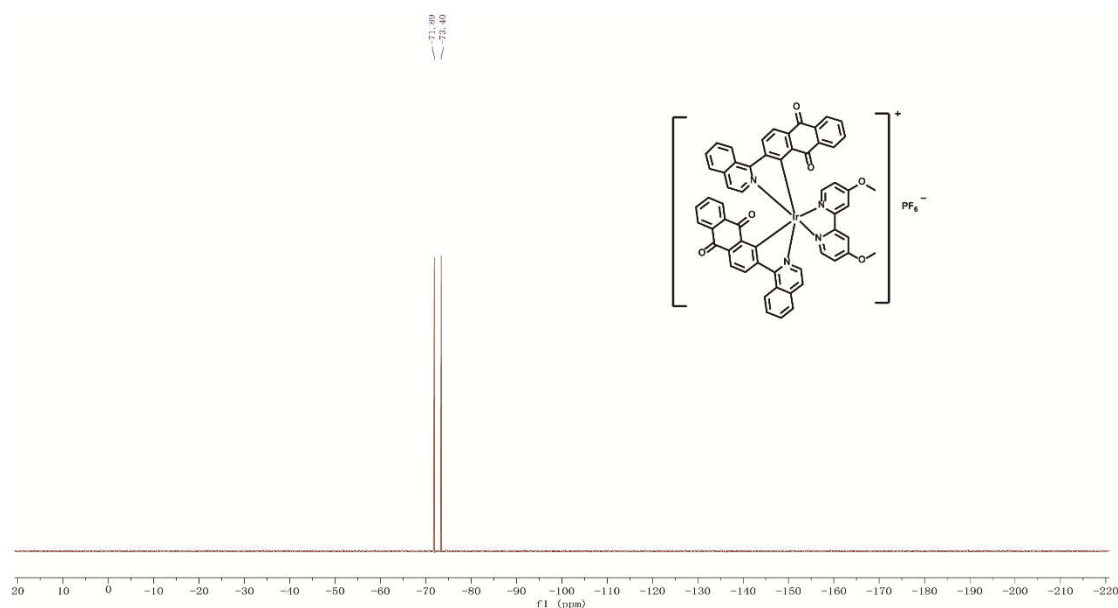
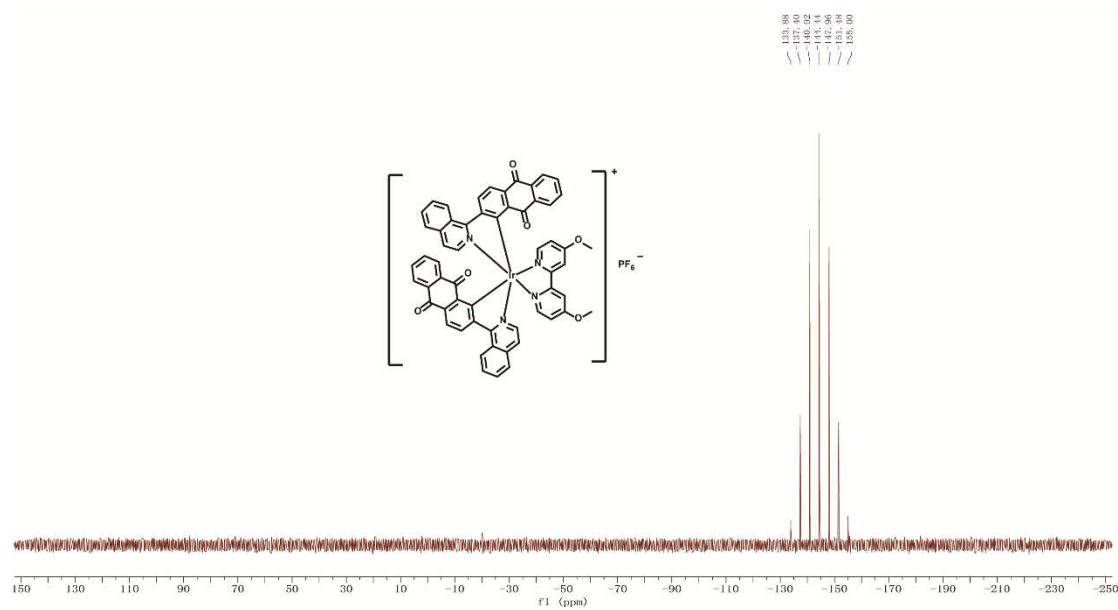


Figure S8. The  $^{13}\text{C}$  NMR spectrum of complex **Ir2**.



**Figure S9.** The  $^{19}\text{F}$  NMR spectrum of complex **Ir2**.



**Figure S10.** The  $^{31}\text{P}$  NMR spectrum of complex **Ir2**.

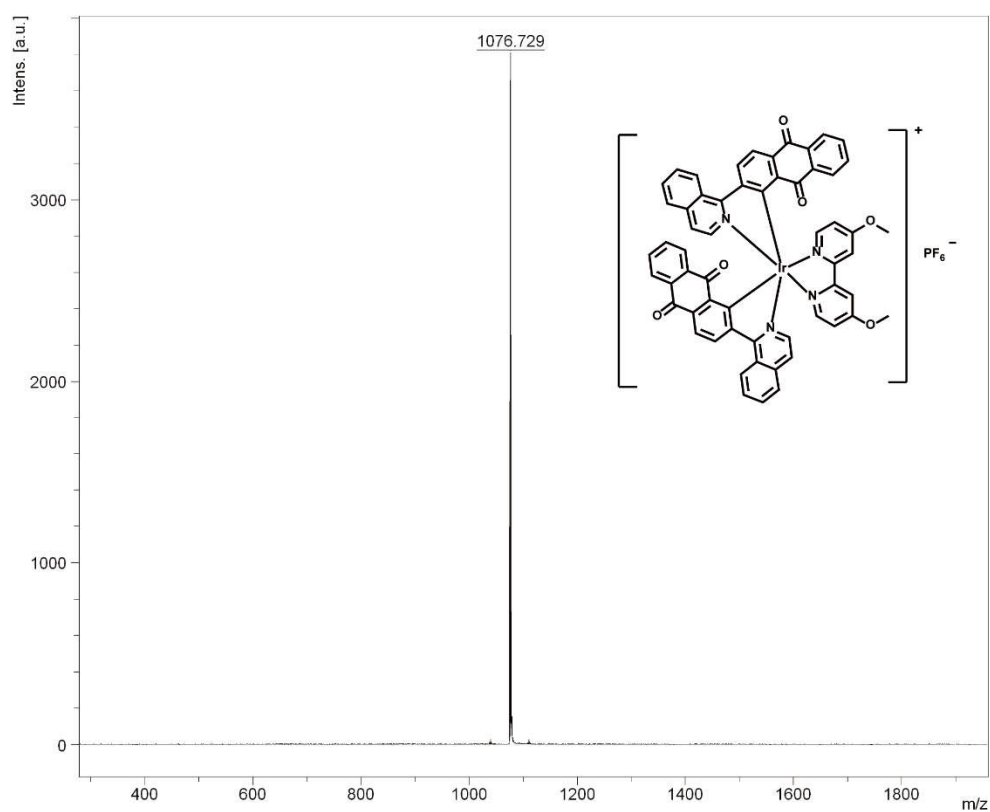


**Figure S11.** MALDI-TOF spectrum of complex **Ir2**.

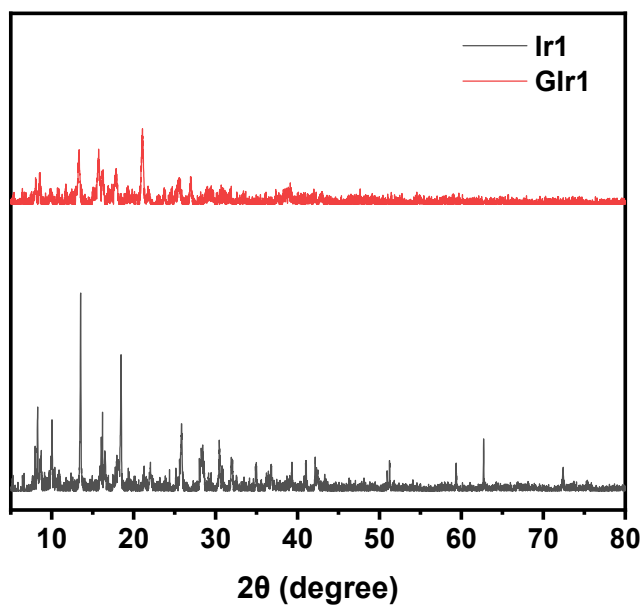


**Figure S12.** PXRD patterns of as-synthesized sample **Ir1** and ground sample **GIr1**.

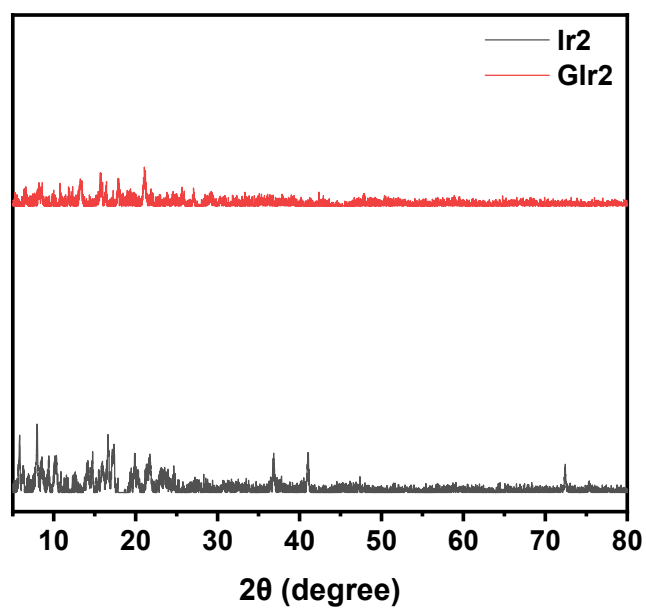


**Figure S13.** PXRD patterns of as-synthesized sample **Ir2** and ground sample **GIr2**.